Homology modelling deduced 3-D structure of *Bacillus thuringiensis Cry*1Ab17 toxin

S. Kashyap[a,*]**, B.D. Singh**[b]**, D.V. Amla**[c]

[a] National Bureau of Agriculturally Important Microorganisms (ICAR), Kusmaur, Kaithouli,
Mau Nath Bhanjan 275101, India

[b] School of Biotechnology, Faculty of Science, Banaras Hindu University, Varanasi 221005 (U.P.) India

[c] Molecular Biology & Genetic Engineering Division, National Botanical Research Institute,
Rana Pratap Marg, P.B. # 436, Lucknow 226001, India

*Corresponding author, e-mail: sudhanshukshyp@gmail.com

ABSTRACT: We predict the first theoretical structural model of the newly reported *Cry*1Ab17 δ-endotoxin produced by *Bacillus thuringiensis* using homology modelling. Both *Cry*1Ab17 and *Cry*1Aa share a common structure; both contain three flexible domains that participate in the formation of a pore and determine the receptor binding specificity. The main differences between the two is in the length of loops, and in *Cry*1Ab17, the absence of α7b, α10a, α10b, α12a, β19, β20 and presence of additional β0 β1b, α9b components. A few of the components such as α8a, α8b, α9a, α9b, and α11a differ in their locations. A better understanding of the 3-D structure of *Cry*1Ab17 will be helpful in designing the domain swapping experiments to improve its insecticidal toxicity.

INTRODUCTION

Insecticidal crystal protein produced by the soil bacterium *Bacillus thuringiensis* (Bt) belongs to a large toxin family with a target spectrum of insects, nematodes, flatworms, and protozoa[1–3], but is currently considered harmless to mammals[3]. The mode of action of *Cry* toxins is still being investigated. The *Cry*1A series of toxins are produced as inactive protoxin within Bt sporangia. On ingestion by a susceptible larva these proteins are proteolytically cleaved to a core toxin fragment that binds to high affinity receptor sites on the midgut membrane. Receptor binding induces conformational changes in the toxin which are necessary for membrane insertion. The inserted toxin disturbs the electrolyte balance by creating pores in the cell membrane leading to cell lysis and finally to larval death[4]. Crystal structures of the active toxins in solutions have been analysed for *Cry*1Aa[5], *Cry*2A[6], *Cry*3A[7], *Cry*3B[8], *Cry*1Ac[9], *Cry*4Ba[10], *Cry*4Aa[11] by X-ray diffraction and while that of *Cry*11Bb[12], *Cry*5Aa[13], *Cry*5Ba[14] have been predicted by homology modelling. The three domains hypothesis[7] states that Domains I, II, and III consist of a bundle of 7 α-helices, antiparallel β-sheets, and a β-sandwich, respectively. Hitherto *Cry*1 toxins have been extensively used in studies aimed to control lepidoptera, but

less attention has been given to their ability to control nematodes or protozoa either alone or in combination. In spite of the above, few studies have examined *Cry*1Ab structure. For a comprehensive understanding of mechanisms underlying insecticidal toxicity, it is imperative to determine the 3-D structures of all the *Cry*1 family members. Here we modelled the *Cry*1Ab17 toxin structure based on the hypothesis of structural similarity[7] with *Cry*1Aa toxin. This model also supports the existing hypotheses of receptor insertion[15] and will further provide initiation into the domain-mutagenesis experiments among *Cry*1 and other toxins for improving their toxicity efficacy.

MATERIALS AND METHODS

Sequence alignment between *Cry*1Ab17 (AAW31761)[16] and *Cry*1Aa1 (PDB 1ciy A) was generated using MEGA[17] (Fig. 1A) and manually checked for correct placement of conserved block elements. The resulting multiple alignments were directly used to jump-start the HHpread interactive server (protevo.eb.tuebingen.mpg.de/hhpred) to detect the protein homology and predict the structure under global alignment mode. The results obtained on-line were manually narrowed down through the choice of a few high scoring entries and

```
  1 YTPIDISLSLTQFLLSEFVPGAGFVLGLVDIIWGIFGPSQWDAFLVQIEQ    50
    |||||||||||||||||||||||||||||||||||||||||||||||||||
  1 YTPIDISLSLTQFLLSEFVPGAGFVLGLVDIIWGIFGPSQWDAFLVQIEQ    50

 51 LINQRIEEFARNQAISRLEGLSNLYQIYAESFREWEADPTNPALREEMRI   100
    |||||||||||||||||||||||||||||||||||||||||||||||||
 51 LINQRIEEFARNQAISRLEGLSNLYQIYAESFREWEADPTNPALREEMRI   100

101 QFNDMNSALTTAIPLLAVQNYQVPLLSVYVQAANLHLSVLRDVSVFGQRW   150
    |||||||||||.||||||||||||||||||||||.||||||||||||||
101 QFNDMNSALTTAIPLFAVQNYQVPLLSVYVQAANLHLPVLRDVSVFGQRW   150

151 GFDAATINSRYNDLTRLIGNYTDYAVRWYNTGLERVWGPDSRDWVRYNQF   200
    |||||||||||||||||||||||:|||||||||||||||||||:|||||
151 GFDAATINSRYNDLTRLIGNYTDHAVRWYNTGLERVWGPDSRDWIRYNQF   200

201 RRELTLTVLDIVALFSNYDSRRYPIRTVSQLTREIYTNPVLENFDGSFRG   250
    ||||||||||:||.||||.||||||||||||||||||||||||||||||
201 RRELTLTVLDIVSLFPNYDSRTYPIRTVSQLTREIYTNPVLENFDGSFRG   250

251 MAQRIEQNIRQPHLMDILNSITIYTDVHRGFNYWSGHQITASPVGFSGPE   300
    .||.||.:||.||||||||||||||.|||..||||||.|||||||||||
251 SAQGIEGSIRSPHLMDILNSITIYTDAHRGEYYWSGHQIMASPVGFSGPE   300

301 FAFPLFGNAGNAAPPV-LVSLTGLGIFRTLSSPLYRRIILGSGPNNQELF   349
    |.|||:|..|||||.. :|:..|.|::|||||.|||...:|.  |||:|.
301 FTFPLYGTMGNAAPQQRIVAQLGQGVYRTLSSTLYRPFNIGI--NNQQLS   348

350 VLDGTEFSFASLTTNLPSTIYRQRGTVDSLDVIPPQDNSVPPRAGFSHRL   399
    ||||||:::.: ::|||||.:||:.||||||||.||||:|:||||.|||||
349 VLDGTEFAYGT-SSNLPSAVYRKSGTVDSLDEIPPQNNNVPPRQGFSHRL   397

400 SHVTMLSQ--AAGAVYTLRAPTFSWQHRSAEFNNIIPSSQITQIPLTKST   447
    |||:|...  :..:|..:.||.||.||:.:||||||||||||||||||||
398 SHVSMFRSGFSNSSVSIIGAPMFSWIHRSAEFNNIIPSSQITQIPLTKST   447

448 NLGSGTSVVKGPGFTGGDILRRTSPGQISTLRVNITAPLSQRYRVRIRYA   497
    |||||||||||||||||||||||||||||||||||||||||||||||||
448 NLGSGTSVVKGPGFTGGDILRRTSPGQISTLRVNITAPLSQRYRVRIRYA   497

498 STTNLQFHTSIDGRPINQGNFSATMSSGSNLQSGSFRTVGFTTPFNFSNG   547
    |||||||||||||||||||||||||||||||||||||||||||||||||
498 STTNLQFHTSIDGRPINQGNFSATMSSGSNLQSGSFRTVGFTTPFNFSNG   547

548 SSVFTLSAHVFNSGNEVYIDRIEFVPAEVT    577
    ||||||||||||||||||||||||||||||
548 SSVFTLSAHVFNSGNEVYIDRIEFVPAEVT    577
```

Fig. 1 Amino acid sequence alignment between *Cry*1Aa and *Cry*1Ab17 sequences. The upper sequence line is of *Cry*1Aa and lower aligned sequence is of *Cry*1Ab17. The similarity (91.9%), gaps (1.0%) and identity (87.8%) between the sequences is calculated with EBLOSUM62 matrix.

HHpread was rerun at local alignment and zero setting. The resultant end alignment was directly fed to MODELLER[18]. The retrieved raw PDB was suitably edited for core toxin molecule using PYMOL 0.99rc6 (www.pymol.org/funding.html), ACCELRYS DS VISUALIZER v2.0.1.7347, and UCSF CHIMERA (www.cgl.ucsf.edu/chimera). The model was validated with PROCHECK[19] by submitting the coordinates to the EMBL- (www.ebi.ac.uk) and ProSA-servers[20] (https: //prosa.services.came.sbg.ac.at). Figures and electrostatic potentials calculation were generated with PyMOL and Ramachandran plot assessment was conducted by submitting the PDB file to RAMPAGE server (mordred.bioc.cam.ac.uk). The final model was submitted to the PMDB database (www.caspur.it/PMDB/) to obtain the PMDB identifier PM0076227.

RESULTS AND DISCUSSION

The reported structural model corresponds with residues 85–662 of the primary structure using the structural based alignment of the amino acid sequence of the *Cry*1Ab17 with *Cry*1Aa1 toxin (Fig. 1). Alignment of Domain I was straightforward and the highly conserved nature of helix 5 in the *Cry*1Ab17 toxin made the placement of the other residues in this domain possible. Alignment of Domain II was also reliable and few manual corrections had to be incorporated within the possible limits of flanking Domains I and III. Domain III of the protein is quite well conserved on the N- and C-terminal sides.

Domain I was composed of N-terminal 257 (85–342) amino acid residues folded into a bundle of 9 amphipathic α-helices and two small β-strands (Table 1). These features are considered highly conserved among the *Cry* toxins[7] and have been proposed to be involved in 'pore formation' by analogy with the helical bundle pore forming structures of colicin A toxin[21] and diphtheria toxin[22]. Evidence from several studies has shown that the central helix (α5) is specifically involved in pore formation[23–25]. All the helices in the *Cry*1Ab17 model were slightly shorter than those in *Cry*1Aa. According to the amphiphilicity calculated with the Hoops and Woods values, the most exposed helices are α1, α2a, α2b, α3, and α6, which correspond well with the accessibility calculated with SWISSPDB, except for α1 which is packed against Domain II. It is possible that this helix has some mobility[26]. The *Cry*1Ab17 Domain I model agrees with data, suggesting that α4 and α5 insert into the membrane in an antiparallel manner reflecting a helical hairpin structure[15]. It is possible that according to the surface electrostatic potential of helices 4 and 5 (Figs. 2 and 3), there is a neutral region in the middle of the helices which probably shows, if the umbrella model is correct, that both helices cross the membrane with their polar sides exposed into the solvent, as is suggested by the results of mutagenesis experiments in the case of the *Cry*1Ac toxin. Mutations in the base of helix 3 and the loop between α3 and α4 cause alterations on the balance of negative charged residues decreasing the toxicity[27]. Mutations in helices α2, α6 and the surface residues of α3 have no important effect on toxicity. Meanwhile, helices α4 and α5 seem to be very sensitive to mutations. Helix α1 probably does not play an important part in toxin activity after the protoxin has been cleaved. It is possible that mutations aimed to increase the amphiphilicity in these helices are anticipated to improve the pore forming activity of *Cry*1Ab17 type toxins.

Table 1 Comparison among three domain structural components of *Cry*1Aa and *Cry*1Ab17 toxin molecules.

Domain I	*Cry*1Aa	*Cry*1Ab17	Domain II	*Cry*1Aa	*Cry*1Ab17	Domain III	*Cry*1Aa	*Cry*1Ab17
α1	Pro35-Ser48	Pro87-Ser100	α8a	Pro271-Glu274	*Ser461-Gly464*	α11a	Leu475-Lys477	*Ser 615-Ser617*
α2a	Aln54-Ile63	Ala106-Trp117	α8b	Ala284-Gln28	*Ser474-Gly477*	β13a	Ser486-Val488	Gly558-Asn566
α2b	Pro70-Ile84	Pro122-Ile136	β2	Asp298-His310	Ile351-His362	β13b	Ile498-Arg 501	Tyr575-Ser583
α3	Glu90-Ala119	Glu142-Ala171	β3	Phe313-Trp316	Glu365-Ser376	β14	Gly505-Asn513	Leu587-Ile593
α4	Pro124-Leu148	Pro176-Phe200	β4	Gly318-Pro325	Arg401-Ala404	β15	Tyr522-Ser530	Arg596-Phe603
α5	Gln154-Trp182	Gln206-Trp234	α9a	Val326-Phe328	*Ala502-His509*	β16	Leu534-Ile540	Arg619-gly622
α6	Ala186-Val218	Ala238-Val270	α9b	—	*Thr524-Pro527*	β17	Arg543-Phe550	Ser633-His641
α7a	Ser223-Thr239	Ser275-Tyr302	β5	Val348-Ser351	Tyr411-Tyr419	α12a	Ser562-Ser564	—
α7b	Leu241-Tyr250	—	β6	Ile357-Arg367	Ser433-Ala441	β18	Arg566-Gly569	Val649-Pro658
β0	—	Ile319-Thr321	β7	Leu380-Leu383	Ala451-Tyr453	β19	Ser580-His588	—
β1a	Glu266-Thr269	Pro323-Asn327	β8	Gly385-Phe390	Thr458-Asp460	β20	Val569-Pro605	—
β1b	—	Ser335-Ser342	β9	Thr400-Tyr402	His480-Phe488			
			α10a	Ser410-Asp412	—			
			α10b	Pro423-Gly426	—			
			β10	His429-Val434	Thr532-Leu534			
			β11	Phe452-His456	Ser539-Val541			
			β12	Thr471-Pro474	Ile551-Arg554			

— similar component not present. *Components in italics are present at downstream sites.
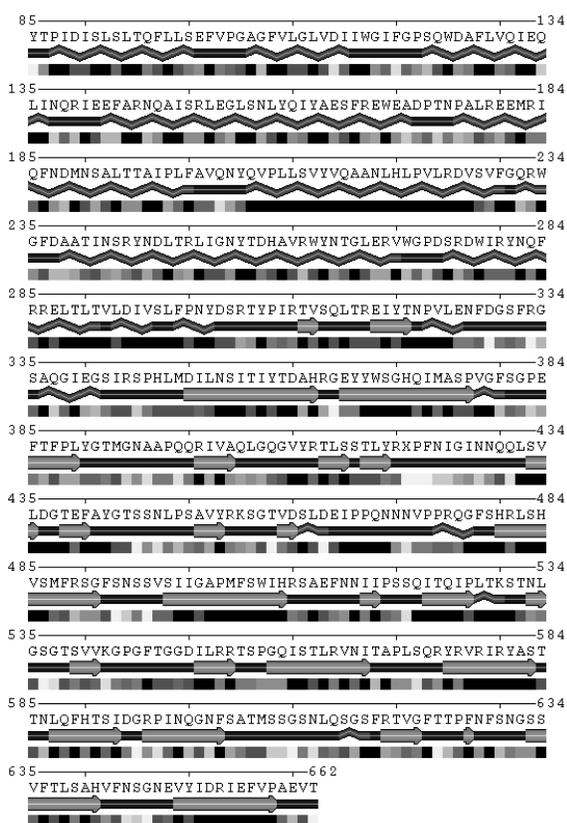

Fig. 2 2-D structure annotation showing sequential arrangements of helices and sheets in *Cry*1Ab17 toxin molecule using POLYVIEW 2D.

As with other *Cry* toxins, Domain II of *Cry*1Ab17 consists of three Greek key β sheets arranged in β prism topology. It comprises residues 343–510, with one helix and 11 β-strands. Domain III is composed of highly conserved residues 523–658. The charge distribution pattern in the theoretical model of *Cry*1Ab17 has a negatively charged patch along β4 and β13 of Domains II and III, respectively. Domain II consists of three anti-parallel β sheets, each ending with exposed loop regions. These loops are thought to participate in receptor binding and hence in determining the specificity of the toxin for attachment on insect receptors. Ge et al[28] managed to alter toxicity of *Cry*1Ac by exchanging the 332–450 amino acids in Domain II with the equivalent segment of *Cry*1Aa. A similar approach has yet to be performed in *Cry*1Ab17. The possibility of regions outside Domain II being involved in receptor recognition was evaluated by mutagenesis into the Domain III loop of *Cry*1Ac. Other regions were also found to be involved in the phenomenon[29]. Chemical modifications of 4 Arg or 7 Tyr residues significantly reduced toxicity and binding[30].

The loops (β2-β3 and β4-β5) probably interact with the receptor through both hydrophobic and electrostatic interactions. This probably helps in receptor binding by providing more mobility to glycine and other similar residues that may interact through salt bridges with the receptor. Loop β4-β5 is mostly hydrophilic and the charged residues at the tip of the loop are probably important determinants for insect specificity. Aromatic amino acids within and adjoining the vicinity of apical loops 2 and 3 of Domain II have been postulated for protein-protein, protein-ligand interactions and have been reported to interact specifically with the outer envelope of the lipid membrane[31]. It has been proposed that these residues interact with hydrophobic lipids tails. The exposed loop architecture has structural affinity for binding to glycoprotein receptors of the target insect
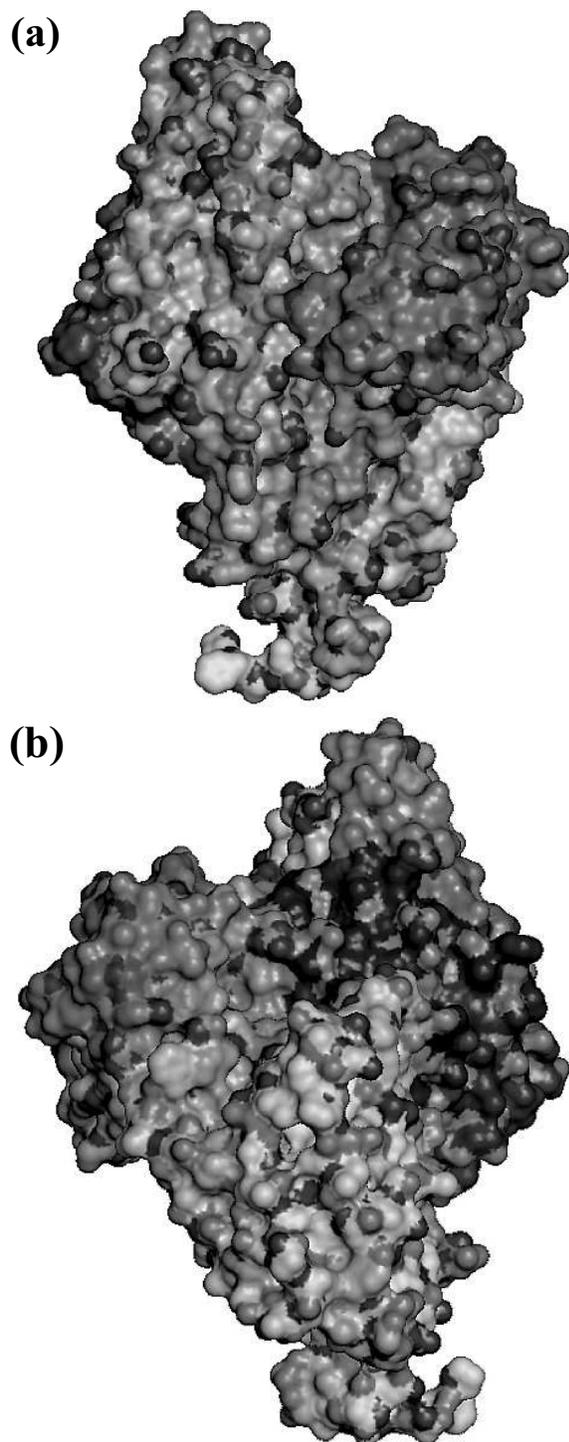
(a)

(b)

Fig. 3 3-D three domain structure of the *Cry*1Ab17 toxin oligomer. (a) Electrostatic potential distribution on the surface of *Cry*1Ab17 toxin molecule. (b) View of the molecule as in (a) after 180° rotation.

membrane[32]. Mutations in defined regions of the *Cry*1Aa toxin (equivalent to residues in the β6-β7 loop of *Cry*1Ab17) have been identified as essential for binding to the membrane of midgut cells of *Bombyx mori*[28, 33]. In the *Cry*1Ab17 model this region is longer than in its counterparts. Loop β2-β3 also seems to be able to modulate the toxicity and specificity of *Cry*1C[34]. The dual specificity of *Cry*2Aa for lepidoptera and diptera insects has been mapped to residues that correspond to the theoretical model of α-sheet 1, strand β6, and the loop between β6-β7 in the *Cry*1Ab17 toxin. Several studies have shown that mutations in the conserved block residues lead to decreased toxicity and alter the channel properties in *Cry*1Ac[7] and *Cry*1Aa[35, 36] toxins.

Finally, the recognition of artefacts and errors in experimental and theoretical structures remain a problem in the field of structure modelling. Web-based software tools like PROSA have a large database and are deployed for the validation of developed models[37]. The software evaluates the model by parsing its coordinates and energy using a distance-based pair potential[38, 39] and capturing the solvent exposed protein residues[38, 39]. The results are displayed in form of a *Z*-score and a plot of residues energy. The *Z*-score shows overall model quality and provides deviations from the random conformation[20, 39]. The plot checks whether the *Z*-score of the protein is within the range of similar proteins (NMR and X-ray derived structures) as in Fig. 4. The value -8.92 is among the native conformation and the overall residues energy was largely negative. The Ramachandran plot showed that most of the modelled residues (93.5%) have φ and ψ angles in the core regions and 4.3% are in allowed regions, except for some proline and glycine residues (1.6%) that fall in the outlier region (Fig. 5). The results for most bond lengths, bond angles, and torsion angles were among the expected values for a naturally folded protein.

Structural comparison of the *Cry*1Aa toxin with the *Cry*1Ab17 model shows correspondence to the general *Cry* protein model (α+β structure with three domains) and the superimposed backbone traces showed low RMS deviations (1.14). This low value shows that the final developed structure has similarity with *Cry*1Aa. This condition is expected since both the sequence has a high homology and the final structure folds are modelled using *Cry*1Aa information. The few differences found were in the sizes of the loops of Domains II and III, length of the two loops joining the apical β-strands (β2-β3 and β4-β5), absence of six components (α7b, α10a, α10b, α12a, β19, β20) and the presence of three additional
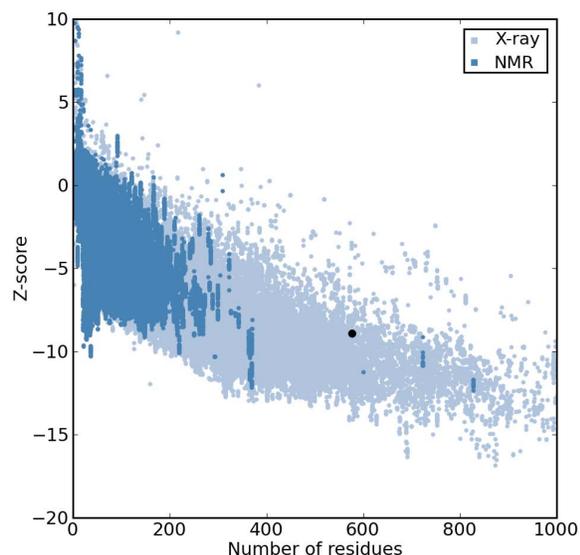
Fig. 4 Model validation of *Cry*1Ac17 with PROSA. The result shows that the structure has features characteristic of native structures. The *Z*-score of −8.92 is highlighted with a large dot.
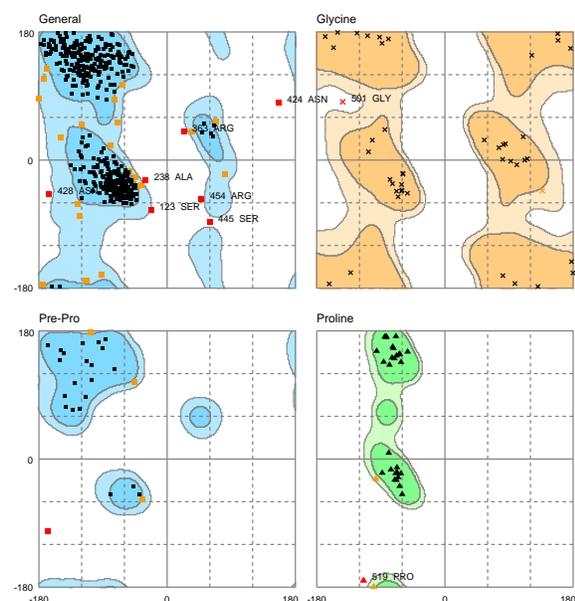

Fig. 5 Ramachandran plot analysis of the *Cry*1Ab17 toxin oligomer showing placement of residues in deduced model. The structure orientation residues are separately considered for angle and torsions. General plot statistics are: residues in most favourable regions 535 (93.4%); residues in additional allowed regions 28 (4.9%); residues in disallowed regions 10 (1.7%). Other plots are evaluated for specific residues as showed at the top left corner of each plot.

β0 β1b, α9b components. Of these, α8a, α8b, α9a, α9b, and α11a are located at different downstream positions (Table 1). We propose that additional and dislocated components have some implications in the specificity of the *Cry*1Ab17 toxin. We presume that residues within these components determine the *Cry*1Ab17 toxin specificity.

REFERENCES

1. Roush RT (1996) Can we slow adaptation by pests to insect transgenic crops? In: Parsley GJ (ed) *Biotechnology and Integrated Pest Management*, CAB International, Willinford, pp 242–63.
2. Roh JY, Choi JY, Li MS, Jin BR, Je YH (2007) *Bacillus thuringiensis* as a specific, safe, and effective tool for insect pest control. *J Microbiol Biotechnol* **17**, 547–59.
3. Schnepf E, Crickmore N, Van Rie J, Lereclus D, Baum J, Feitelson J, Zeigler DR, Dean DH (1998) *Bacillus thuringiensis* and its pesticidal crystal proteins. *Microbiol Mol Biol Rev* **62**, 772–806.
4. Hofmann C, Vanderbruggen H, Höfte H, Van Rie J, Jensens S, Van Mellaert H (1988) Specificity of *Bacillus thuringiensis* δ-endotoxins is correlated with the presence of high-affinity binding sites in the brush border membrane of target insect midgets. *Proc Natl Acad Sci USA* **85**, 7844–8.
5. Knowles BH, Ellar DJ (1987) Colloid osmotic lysis is a general feature of the mechanism of action of *Bacillus thuringiensis* δ-endotoxins with different insect specificities. *Biochim Biophys Acta* **924**, 509–18.
6. Morse RJ, Yamamoto T, Stroud RM (2001) Structure of Cry2Aa suggests an unexpected receptor binding epitope. *Structure* **9**, 409–17.
7. Li J, Carroll J, Ellar DJ (1991) Crystal structure of insecticidal δ-endotoxin from *Bacillus thuringiensis* at 2.5 Åresolution. *Nature* **353**, 815–21.
8. Galitsky N, Cody V, Wojtczak A, Ghosh D, Luft JR, Pangborn W, English L (2001) Structure of the insecticidal bacterial δ-endotoxin *Cry*3Bb1 of *Bacillus thuringiensis*. *Acta Crystallogr D* **57**, 1101–9.
9. Derbyshire DJ, Ellar DJ, Li J (2001) Crystallization of the *Bacillus thuringiensis* toxin *Cry*1Ac and its complex with the receptor ligand *N*-acetyl-D-galactosamine. *Acta Crystallogr D* **57**, 1938–44.
10. Boonserm P, Davis P, Ellar DJ, Li J (2005) Crystal structure of the mosquito-larvicidal toxin *Cry*4Ba and its biological implications. *J Mol Biol* **348**, 363–82.
11. Boonserm P, Mo M, Angsuthanasombat C, Lescar J (2006) Structure of the functional form of the mosquito larvicidal *Cry*4Aa toxin from *Bacillus thuringiensis* at a 2.8-Angstrom resolution. *J Bacteriol* **188**, 3391–401.

12. Gutierrez P, Alzate O, Orduz S (2001) A theoretical model of the tridimensional structure of *Bacillus thuringiensis* subsp. *medellin* Cry11Bb toxin deduced by homology modeling. *Mem Inst Oswaldo Cruz* **96**, 357–64.

13. Min ZX, Qui XL, Zhi DX, Xiang WF (2009) The theoretical three-dimensional structure of *Bacillus thuringiensis Cry*5Aa and its biological implications. *Protein J* **28**, 104–10.

14. Xia LQ, Zhao XM, Ding XZ, Wang FX, Sun YJ (2008) The theoretical 3D structure of *Bacillus thuringiensis Cry*5Ba. *J Mol Model* **14**, 843–8.

15. Gazit E, La Rocca P, Sansom MSP, Shai Y (1998) The structure and organization within the membrane of the helices composing the pore forming domain of *Bacillus thuringiensis* δ-endotoxin are consistent with an "umbrella-like" structure of the pore. *Proc Natl Acad Sci USA* **95**, 12289–94.

16. Zhong WF, Fang JC, Guo HF, Liu BS, Wang JP, Zhu YX, Du ZW (2005) Screening of *Bacillus thuringiensis* strain with broad spectrum and high toxicity and cloning of its insecticidal crystal protein gene. *Hua Nan Nong Ye Da Xue Xue Bao* **26**, 40–2.

17. Tamura K, Dudley J, Nei M, Kumar S (2007) MEGA4: Molecular evolutionary genetics analysis (MEGA) software version 4.0. *Mol Biol Evol* **24**, 1596–9.

18. Sali A, Potterton L, Yuan F, van Vlijmen H, Karplus M (1995) Evaluation of comparative protein modeling by MODELLER. *Protein Struct Funct Genet* **23**, 318–26.

19. Laskowski RA, MacArthur MW, Moss DS, Thornton JM (1993) PROCHECK: a program to check the stereochemical quality of protein structures. *J Appl Crystallogr* **26**, 283–91.

20. Sippl MJ (1993) Recognition of errors in three-dimensional structures of proteins. *Protein Struct Funct Genet* **17**, 355–62.

21. Parker MW, Pattus F, Tucker AD, Tsernoglou D (1989) Structure of the membrane-pore-forming fragment of colicin A. *Nature* **337**, 93–6.

22. Choe S, Bennett MJ, Fujii G, Curmi PMG, Kantardjieff KA, Collier RJ, Eisenberg D (1992) The crystal structure of diphtheria toxin. *Nature* **357**, 216–22.

23. Ahamad W, Ellar DJ (1990) Directed mutagenesis of selected regions of a *Bacillus thuringiensis* entomocidal protein. *FEMS Microbiol Lett* **68**, 97–104.

24. Wu D, Aronson AI (1992) Localised mutagenesis defines regions of the *Bacillus thuringiensis* δ-endotoxin involved in toxicity and specificity. *J Biol Chem* **26**, 2311–7.

25. Gazit E, Shai Y (1993) Structural and functional characterization of the α5 segment of *Bacillus thuringiensis* δ-endotoxin. *Biochemistry* **32**, 3429–36.

26. Segura C, Guzman F, Patarroyo ME, Orduz S (2000) Activation pattern and toxicity of the Cry11Bb1 toxin of *Bacillus thuringiensis* subsp. *medellin*. *J Invertebr Pathol* **76**, 56–62.

27. Kumar ASM, Aronson AI (1999) Analysis of mutations in the pore-forming region essential for insecticidal activity of a *Bacillus thuringiensis* δ-endotoxin. *J Bacteriol* **181**, 6103–7.

28. Ge AZ, Shivarova NI, Dean DH (1989) Location of the *Bombyx mori* specificity domain of a *Bacillus thuringiensis* δ-endotoxin protein. *Proc Natl Acad Sci USA* **86**, 4037–41.

29. Aronson AI, Wu D, Zhang C (1995) Mutagenesis of specificity and toxicity regions of a *Bacillus thuringiensis* protoxin gene. *J Bacteriol* **177**, 4059–65.

30. Cummings CE, Ellar DJ (1994) Chemical modification of *Bacillus thuringiensis* activated δ-endotoxin and its effect on toxicity and binding to *Manduca sexta* midgut membranes. *Microbiology* **140**, 2737–47.

31. Bressanelli S, Stiasny K, Allison SL, Stura EA, Duquerroy S, Lescar J, Heinz FX, Rey FA (2004) Structure of a flavivirus envelope glycoprotein in its low-pH-induced membrane fusion conformation. *EMBO J* **23**, 728–38.

32. Griffitts JS, Haslam SM, Yang T, Garczynski SF, Mulloy B, Morris H, Cremer PS, Dell A, Adang MJ, Aroian RV (2005) Glycolipids as receptors for *Bacillus thuringiensis* crystal toxin. *Science* **307**, 922–5.

33. Lu H, Rajamohan F, Dean DH (1994) Identification of amino acid residues of *Bacillus thuringiensis* δ-endotoxin *Cry*IAa associated with membrane binding and toxicity to *Bombyx mori*. *J Bacteriol* **176**, 5554–9.

34. Smith GP, Ellar DJ (1994) Mutagenesis of two surface exposed loops of the *Bacillus thuringiensis Cry*IC δ-endotoxin affects insecticidal specificity. *Biochem J* **302**, 611–6.

35. Chen XJ, Lee MK, Dean DH (1993) Site-directed mutations in a highly conserved region of *Bacillus thuringiensis* δ-endotoxin affect inhibition of short circuit current across *Bombyx mori* midguts. *Proc Natl Acad Sci USA* **90**, 9041–5.

36. Schwartz JL, Potvin L, Chen XJ, Brousseau R, Laprade R, Dean DH (1997) Single-site mutations in the conserved alternating-arginine region affect ionic channels formed by *Cry*IAa, a *Bacillus thuringiensis* toxin. *Appl Environ Microbiol* **63**, 3978–84.

37. Wiederstein M, Sippl MJ (2007) ProSA-web: interactive web service for the recognition of errors in three-dimensional structures of proteins. *Nucleic Acids Res* **35**, W407–10.

38. Sippl MJ (1990) Calculation of conformational ensembles from potentials of mean force: An approach to the knowledge-based prediction of local structures in globular proteins. *J Mol Biol* **213**, 859–83.

39. Sippl MJ (1995) Knowledge-based potentials for proteins. *Curr Opin Struct Biol* **5**, 229–35.